ISSN 1674-1056
http://cpb.iphy.ac.cn
http://iopscience.iop.org/cpb
中国物理 B
Chinese Physics
中国物理 Chinese Physics B

Characterization of focusing performance of spiral zone plates with fractal structure

Hua-Ping Zang(臧华平), Cheng-Long Zheng(郑程龙), Zi-Wen Ji(吉子雯), Quan-Ping Fan(范全平), Lai Wei(魏来), Yong-Jie Li(李永杰), Kai-Jun Mu(牧凯军), Shu Chen(陈述), Chuan-Ke Wang(王传珂), Xiao-Li Zhu(朱效力), Chang-Qing Xie(谢常青), Lei-Feng Cao(曹磊峰), Er-Jun Liang(梁二军)

Citation: Chin. Phys. B . 2019, 28(6): 064201. **doi:** 10.1088/1674-1056/28/6/064201
Journal homepage: http://cpb.iphy.ac.cn; http://iopscience.iop.org/cpb

What follows is a list of articles you may be interested in

Numerical study of optical trapping properties of nanoparticle on metallic film with periodic structure

Cheng-Xian Ge(葛城显), Zhen-Sen Wu(吴振森), Jing Bai(白靖), Lei Gong(巩蕾)
Chin. Phys. B . 2019, 28(2): 024203. **doi:** 10.1088/1674-1056/28/2/024203

High efficiency terahertz diffraction grating with trapezoidal elements

Yin-Zhong Wu(巫殷忠), Quan-Pin Fan(范全平), Qiang-Qiang Zhang(张强强), Lai Wei(魏来), Yong Chen(陈勇), Zu-Hua Yang(杨祖华), Lei-Feng Cao(曹磊峰)
Chin. Phys. B . 2017, 26(12): 124203. **doi:** 10.1088/1674-1056/26/12/124203

Orbital angular momentum density and spiral spectra of Lorentz-Gauss vortex beams passing through a single slit

Zhi-Yue Ji(季志跃), Guo-Quan Zhou(周国泉)
Chin. Phys. B . 2017, 26(9): 094202. **doi:** 10.1088/1674-1056/26/9/094202

Difference scattering field properties between periodic defect particles and three-dimensional slightly rough optical surface

Cheng-Xian Ge(葛城显), Zhen-Sen Wu(吴振森), Jing Bai(白靖), Lei Gong(巩蕾)
Chin. Phys. B . 2017, 26(6): 064201. **doi:** 10.1088/1674-1056/26/6/064201

Quantum-mathematical model of edge and peak point in Fresnel diffraction through a slit

Xiao-He Luo(罗晓贺), Hui Mei(惠梅), Qiu-Dong Zhu(朱秋东), Shan-Shan Wang(王姗姗), Yin-Long Hou(侯银龙)
Chin. Phys. B . 2017, 26(5): 054202. **doi:** 10.1088/1674-1056/26/5/054202

Characterization of focusing performance of spiral zone plates with fractal structure*

Hua-Ping Zang(臧华平)[1], Cheng-Long Zheng(郑程龙)[1], Zi-Wen Ji(吉子雯)[1], Quan-Ping Fan(范全平)[2], Lai Wei(魏来)[2], Yong-Jie Li(李永杰)[3], Kai-Jun Mu(牧凯军)[1], Shu Chen(陈述)[1], Chuan-Ke Wang(王传珂)[2], Xiao-Li Zhu(朱效力)[4], Chang-Qing Xie(谢常青)[4], Lei-Feng Cao(曹磊峰)[2,†], and Er-Jun Liang(梁二军)[1,‡]

[1] *School of Physics Science and Engineering, Zhengzhou University, Zhengzhou* 450001, *China*
[2] *National Key Laboratory for Laser Fusion, Research Center of Laser Fusion, China Academy of Engineering Physics, Mianyang* 621900, *China*
[3] *Information and Telecommunication Company of State Grid Henan Electric Power Corporation, Zhengzhou* 450001, *China*
[4] *Key Laboratory of Nano-Fabrication and Novel Devices Integrated Technology, Institute of Microelectronics, Chinese Academy of Sciences, Beijing* 100029, *China*

(Received 2 December 2018; revised manuscript received 21 February 2019; published online 8 May 2019)

We propose an efficient method of generating a vortex beam with multi-foci by using a fractal spiral zone plate (FSZP), which is designed by combining fractal structure with a spiral zone plate (SZP) in the squared radial coordinate. The theoretical analysis reveals that the number of foci that embed vortices is significantly increased as compared with that obtained by using a conventional SZP. Furthermore, the influence of topological charge on the intensity distribution in focal plane is also discussed in detail. For experimental investigation, an FSZP with topological charge $p = 1$ and 6.4 mm diameter is fabricated by using a photo-etching technique. The calibration indicates that the focusing performances of such a kind of zone plane (ZP) accord well with simulations, thereby providing its potential applications in multi-dimensional optical manipulation and optical imaging technology.

Keywords: optical vortices, spiral zone plate, diffractive optical elements

PACS: 42.25.Fx, 42.79.–e, 42.79.Ag, 42.79.Ci **DOI:** 10.1088/1674-1056/28/6/064201

1. Introduction

An optical vortex beam, which carries orbital angular momentum (OAM), has aroused increasingly the research interest because of its wide potential applications, ranging from optical manipulation[1,2] to optical communication in free-space.[3] The spatial distribution wave front of a vortex beam can be described as $\exp(\mathrm{i}p\varphi)$, where p is the topological charge (TC) and φ represents the azimuth angle. Various diffractive optical elements, such as vortex encoding gratings,[4] holographic gratings,[5] binary phase Fresnel zone plates,[6] spiral phase plate (SPP),[7,8] and spiral zone plate (SZP)[9,10] have been used to generate optical vortices. In particular, SZP offers great advantages of compactness, light weight, high alignment, and high degree of design flexibility. Optical vortex beam generated by a computer-generated SZP has been demonstrated in Ref. [11]. However, the focused vortex diverges rapidly after passing through the focal plane since a conventional zone plate provides only one focal spot for one shot of laser beam, which greatly limits the scope of applications. Therefore, many different kinds of generators for beams with multiple optical vortices have been proposed recently, such as a vortex grating[12] and a three-dimensional (3D) twister superlattice embedded with vortex spirals.[13]

Fractal zone plate (FZP) is a meaningful method of producing a sequence of focal planes and the internal structure of each focus exhibits a characteristic fractal structure.[14] In 2006, Tao *et al.*[15] and Cheng *et al.*[16] proposed a new family of zone plate named spiral fractal zone plates by combining the phase modulation function of helical phase structure and the properties of the FZP to generate a series of focused optical vortices along the propagation direction. In addition, it has been reported that different aperiodic zone plates combined with a vortex lens could produce a chain of vortices with tunable separation, strength and transverse section.[17] However, the fabrication of a perfect helical phase structure with the required surface variation is a challenge for the current production technology. More recently, Yu *et al.*[18] presented a kind of spiral Dammann zone plate with a binary structure to generate a coaxial dipole vortex array. However, in an optical system, a focusing objective must be placed after this zone plate, which may be difficult for working in the extreme ultraviolet or x-ray regions.

In this paper, we present a technique for producing a se-

*Project supported by the National Natural Science Foundation of China (Grant Nos. 11404290 and 61505178), the Major National Scientific Instruments Developing Special Project (Grant No. 2012YQ130125), the Postdoctoral Science Foundation of Henan Province, China (Grant No. 2013008), the Program for Science & Technology Innovation Talents in Universities of Henan Province, China (Grant No. 172102210481), and the Key Scientific Research Projects in Universities of Henan Province, China (Grant No. 19B140005).

†Corresponding author. E-mail: leifeng.cao@caep.cn
‡Corresponding author. E-mail: ejliang@zzu.edu.cn

© 2019 Chinese Physical Society and IOP Publishing Ltd

ries of optical vortices along the optical axis based on a simple compact system by using binary fractal spiral zone plates (FSZP). The key idea of the proposed FSZP is to combine the advantages of SZP and Cantor fractal structure along the square of the radial coordinates together. Unlike the phase-only zone plate loaded onto the SLM in Ref. [19], the design and fabrication by applying an electron beam lithography to the FSZP are presented and the corresponding axial irradiance is examined. An FSZP with 6.4-mm diameter and 0.2-m focal-length is fabricated by photo-etching technology. We also demonstrate the observation of generating optical vortices with different TCs. This ZP is meaningful for various areas, and the typical binary structure will be beneficial to multi-wavelength application.

2. Design

The SZP can be considered as a variation of Fresnel zone plate combined with radial Hilbert transform (RHT) filtering operation. Therefore, the phase function of the SZP can be expressed as

$$\mathrm{SZP}(r,\varphi)=\exp\left(\mathrm{i}p\varphi-\frac{\mathrm{i}\pi r^2}{\lambda f}\right), \tag{1}$$

where p represents the TC, $(r,\ \varphi)$ are the polar coordinates, f is the focal length of the SZP corresponding to the wavelength of incident light λ. The phase function in Eq. (1) can be binarized into a binary transmittance function as follows:

$$t(r,\theta)=\begin{cases}1,\ (3-2\,m)\pi\le p\varphi-\dfrac{\pi r^2}{\lambda f}<(4-2\,m)\pi,\\ 0,\ \text{else},\end{cases}$$
$$m=1,2,3,\ldots, \tag{2}$$

where m represents the number of zones. From Eq. (2), we obtain an SZP in the (x,y) coordinate and an SZP in $(r^2,\ \varphi)$ coordinate as shown in Fig. 1(a) where TC $p=1$. It can be seen that the alternating opaque and transparent zones of a conventional SZP are evenly spaced in the polar coordinate system. Inspired by the principle of FZP, we construct the FSZP by selecting some clear zones of SZP to make it accord with the fractal structure along the square of the radial coordinate. In this case, we choose a regular Cantor-fractal structure for our design, and the transmittance function of FSZP can be expressed as

$$t(r,\theta)=\begin{cases}1,\quad (1-a(k))\pi\le p\varphi-\dfrac{\pi r^2}{\lambda f}<(2-a(k))\pi,\\ 0,\quad \text{else},\end{cases}$$
$$k=1,2,\ldots,N^S. \tag{3}$$

If $N=2$,

$${}^Sa(k)=\begin{cases}0, & k=1,\\ 2, & k=2,\\ {}^{S-1}a(k), & k\le 2^{S-1},\\ {}^Sa(k-2^{S-1})+2({}^Sa(2^{S-1})+1), & k>2^{S-1},\end{cases}$$
$$k=1,2,\ldots,N^S, \tag{4}$$

where S and N represent the fractal stage and the number of segments of the fractal structure, respectively, which are the most essential parameters of the Cantor fractal structure. The evolution and modulation of these two parameters are important for controlling the number of focused vortices. And $a(k)$ is a sequence representing the start position of the reserved zones according to the Cantor fractal structure. The structure of an FSZP with $p=1$, $N=2$, $S=3$ is shown in Fig. 1(b). In the view of (x,y) coordinate system, an FSZP looks like a fragmentary SZP but the former one is characterized not only by a binary helical structure but also by a fractal structure.

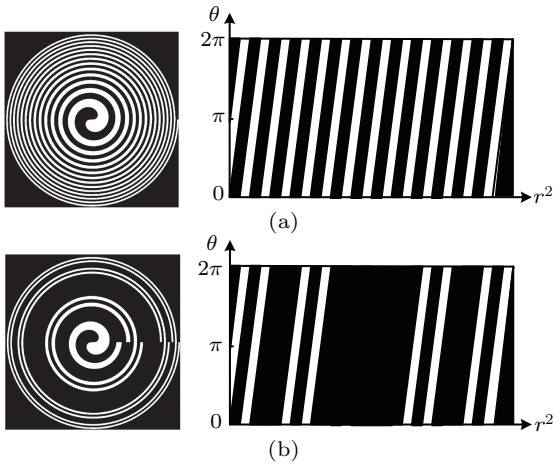


Fig. 1. Schematic view of zone plate in $(r^2,\ \theta)$ coordinate system and (x,y) coordinate system (a) SZP with $p=1$, $m=14$; (b) FSZP with $p=1$, $N=2$, $S=3$.

Table 1. Fabrication parameters.

Focal distance	200 mm
Wavelength	632 nm
Last zone width	19.75 μm
Diameter	6.4 mm
Number of zones	41
Thickness	2.25 mm
Membrane	chromium layer
Substrate	soda-lime glass

The fabrication process of FSZP by using the photo etching technique is similar to that of conventional binary SZP. To obtain a better focusing performance, in this work a specific FSZP with $p=1$, $N=2$, and $S=4$ was fabricated with the processing parameters in Table 1 based on the photo-etching technique. As illustrated in Fig. 2(a), the fabrication process consists of four main steps. First, a 100-nm-thick chromium layer was spin-coated on a 2.25-mm-thick soda-lime glass substrate, sequentially photoresist (AZ1500, AZ electronic materials, USA) with a thickness of 500-nm was spin-coated onto it. Then, the FSZP pattern formed on the photo resist which was placed in a direct writing laser at a wavelength of 413 nm (DWL 2000, Heidelberg Instruments,

Germany) and developed in a 6-wt‰ sodium hydroxide solution. After exposure, the opening parts of the chromium layer were removed by using a chromium etchant to transfer the pattern from the photoresist to the chromium layer. Finally, we removed the remaining resist by using chemicals. The microstructure image of the obtained FSZP is shown in Fig. 2(b).

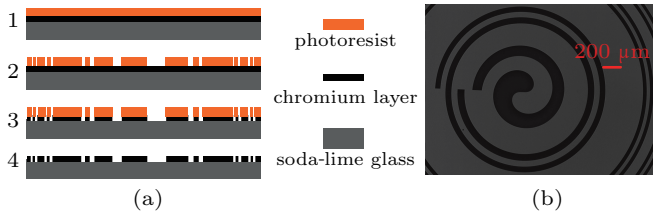


Fig. 2. (a) Schematic flow chart of fabrication process of FSZPs which consists of 1 chromium layer and photoresist coatings, 2 exposure, 3 chromium etching, and 4 resist removal; (b) microscopic image of fabricated FSZP sample.

3. Simulations

The FSZP can be used as a single element objective to optically implement the radial Hilbert filtering operation and the Fresnel zone plate focusing operation in one step. Therefore, numerical simulations for the focusing characteristics of FSZP can be performed by using the Fresnel–Kirchhoff diffraction equation based on the scalar diffraction theory. The distribution of complex amplitude $U(\xi,\eta)$ after diffractive plane can be expressed as

$$U(\xi,\eta) = \frac{A}{\mathrm{j}\lambda}\frac{\exp(\mathrm{j}kR')}{R'}\int_0^{2\pi}\int_0^{2\pi} t(r,\phi)\left[\frac{z/R+1}{2}\right] \times \frac{\exp(\mathrm{j}kR)}{R} r\,\mathrm{d}r\,\mathrm{d}\phi, \tag{5}$$

where A is a constant, $t(r,\varphi)$ represents the transmittance of the FSZP, $k = 2\pi/\lambda$ represents the wave number, R' is the distance from the source to a point on the zone plate, and R is the distance between the observation point to the zone plate. After calculating the complex amplitude, the light strength distribution $I(\xi,\eta)$ can be obtained from $I(\xi,\eta) = |U(\xi,\eta)|^2$.

To verify our design and evaluate the advantage of FSZPs by increasing the depth of focus, we compare the axial intensity distribution of an FSZP with a corresponding SZP under the same circumstance. Here, these parameters are chosen to be $\lambda = 632$ nm, $f = 200$ mm, $p = 1$, $N = 2$, and $S = 4$. As shown in Figs. 3(a) and 3(b), we can see that doughnut-shape patterns are achieved in the primary focal plane for both SZP and FSZP. The difference is that a series of subsidiary vortices in the other focal planes (180, 193, 207, and 225 mm, respectively) for FSZP can be clearly observed, which is considered as splitting from the primary focus. With the increase of the s value, the number of subsidiary foci increases, with the whole axial range unchanged, which is $2n-1$ times higher than the number of subsidiary foci in the previous fractal structure. Other major foci that are also surrounded by subsidiary foci appear at distances of $f/7$, $f/5$, and $f/3$ have also been observed in this process. Figures 3(c) and 3(d) show the diffraction patterns of the SZP and FSZP at calculated focal planes, from which we can clearly see that the SZP beam is divergent quickly at positions before or after focal length. In contrast, the vortices of FSZP beam have almost the same size at the plane of the primary focus as those for the cases of the other four subsidiary foci.

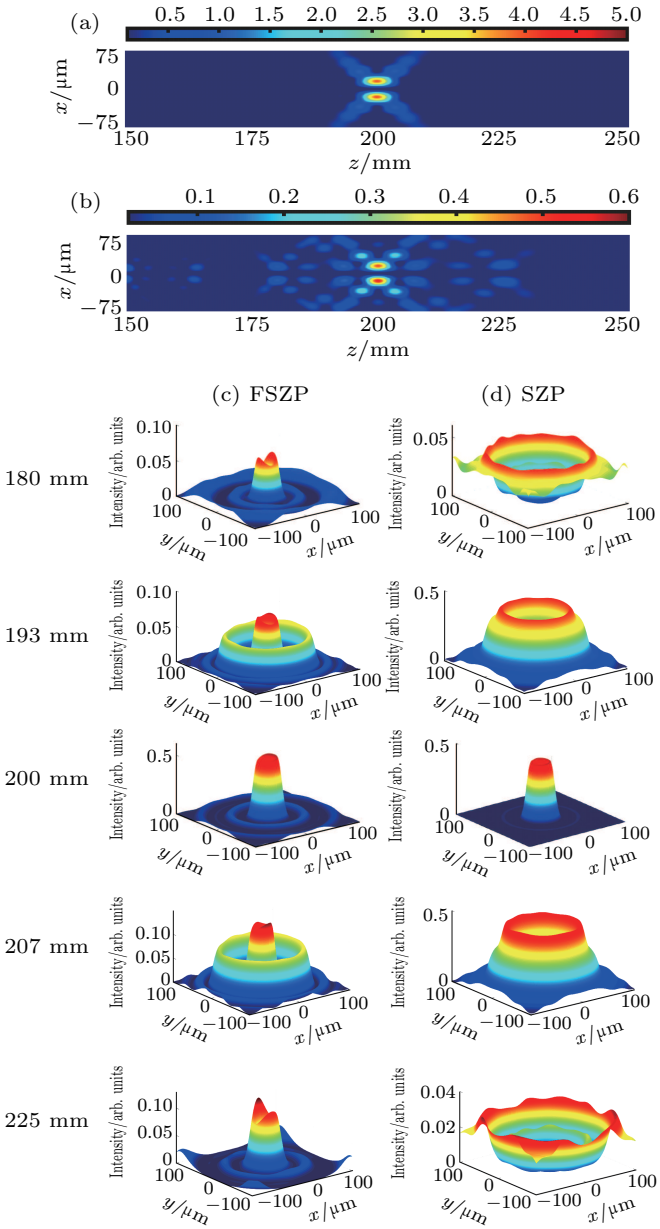


Fig. 3. Intensity distribution of (a) SZP with $p = 1$, (b) FSZP with $p = 1$, $N = 2$, $S = 4$, and calculated cross-section irradiance of (c) FSZP and (d) SZP.

The central point of the optical vortex is called a singular point because of the undefined phase and zero intensity.[20] Around the dark core, each focus of FSZP beam as shown in Fig. 3(c) exhibits the variation of a helical phase that is an integer multiple of 2π. Therefore, the phase distribution of optical

vortices can be expressed as $\exp(\mathrm{i}p\varphi)$ under the paraxial approximation, and the intensity of OAM is $p\hbar$. The value of TC has a great influence on the characteristics of optical vortices. Figure 4 shows the FSZP with different TCs and the calculated intensities of light fields on the first subsidiary focal plane, the main focal plane and the second subsidiary focal plane, respectively. Noticeably, here we normalized the intensity patterns for better exhibiting the results. In the case of $p = 1$, the foci present bright rings with uniformity and symmetry at the main and subsidiary focal plane. Generations of higher order TC $p = 2$ are shown in the middle line of Fig. 4, where relatively large bright intensity rings are captured in the main focal plane. However, the two subsidiary foci have a tendency to break down into two lobes due to the particular helical phase structures of optical vortices. As the value of TC increases to $p = 3$, the size of main focus keeps growing and the phase variations of subsidiary foci are more obvious. Such optical vortex beams can trap or guide particles in their dark center or drive particles to spin by transferring the angular momentum to them.[21]

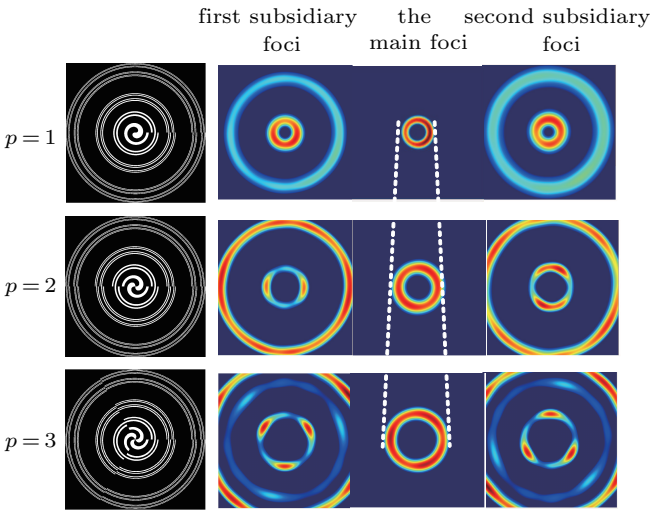


Fig. 4. Diffraction patterns of the main and subsidiary foci for FSZP with different TCs.

4. Experiment

Experiments were carried out by using the fabricated zone plate and the experimental arrangement is shown schematically in Fig. 5(a). The incident light with a wavelength of 632 nm was expanded and collimated by a collimator lens to illuminate the FSZP sample. The uniform parallel light was then modulated by the FSZP and then focused on the focal planes. A charge-coupled device (CCD) (Lumenera Infinity, 2048×2448, 3.45 μm×3.45 μm/pixel) camera was located on a sliding guide behind the FSZP to record the intensity distributions of reconstructed beam at different positions. It should be noted that a filter should be placed in front of the CCD to avoid the camera from becoming saturated. To make a direct comparison with simulation, we recorded the cross-section intensities of the FSZP beam away from 150 mm to 250 mm for 100 images at different positions. Figure 5(b) shows the recovered axial irradiances of the FSZP along the propagation direction. As expected, a beam with sequence of vortex foci was generated by the fabricated FSZP. To further validate the experimental data, figure 5(c) presents the comparison curves of the intensity distributions obtained from the experiment and simulation with the same parameters. Typically, we take the curves crossing over the most intense center of the vortex in the focal plane of the primary focus to represent the distribution of foci due to the same size of sequence vortices along the propagation direction at different focal positions. Overall, the experimental characteristics of generation accord with simulations considering that the only difference in the similar diffraction feature (such as the same positions and sizes of the main and subsidiary foci) is a relatively high background noise, which may be caused by the interference of the external light in the laboratory.

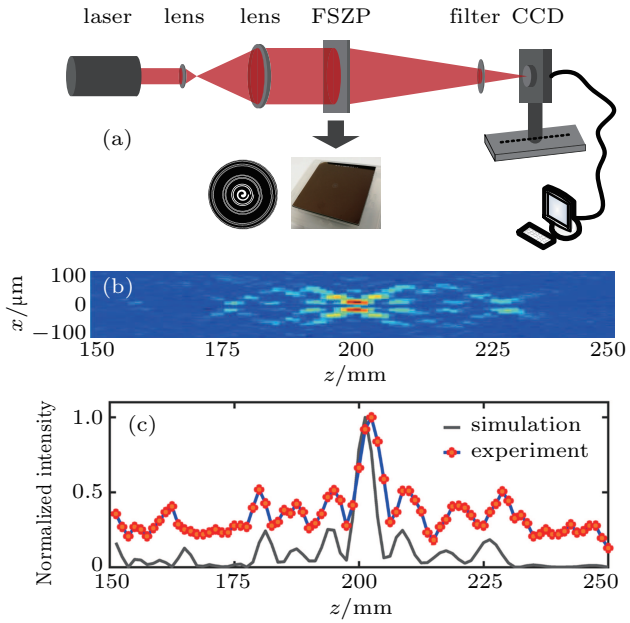


Fig. 5. (a) Schematic diagram of experimental setup; (b) longitudinal intensity distribution on meridian plane; (c) measured normalized peak intensity distribution of vortex ring along e optical axis.

The captured intensity distributions for focused vortices at different positions of the FSZP beam are shown in Fig. 6(a). As expected, the main focus that is located at 200 mm exhibits a uniform intensity distribution while the other four subsidiary foci are founded at 178, 194, 206, and 227 mm, respectively. As the beam spreads along the propagation direction, the sizes of the optical vortices stay almost the same within the whole focal volume, which can be explained as an extension of the depth of focus. The detailed characteristics of the main focus of the FSZP are shown in Fig. 6(b), the marks represent each pixel of the CCD. As we can see, the two peaks are completely symmetric and the radius of the doughnut pattern is about 20 μm. A comparison shows that the experimental results

including the number of foci and size of the vortices are in good agreement with the simulations, in which the limitation of the CCD resolution (3.45 μm×3.45 μm/pixel) is taken into account. In the calibration, experimental errors can emerge, which are related to the instability of the light source, the accuracies of the instruments, and the recovery of the vortex beam. Figure 6(c) shows the curves of normalized intensity profiles of the obtained main focus and subsidiary foci along the longitudinal axis. Obviously, the curves are fitted well with each other, implying that the sequence optical vortices generated by FSZP exhibit almost constant lateral dark core sizes. Therefore, we anticipate that FSZP can provide a complementary and versatile high-resolution nondestructive tool for particle manipulation and microscope imaging.[22]

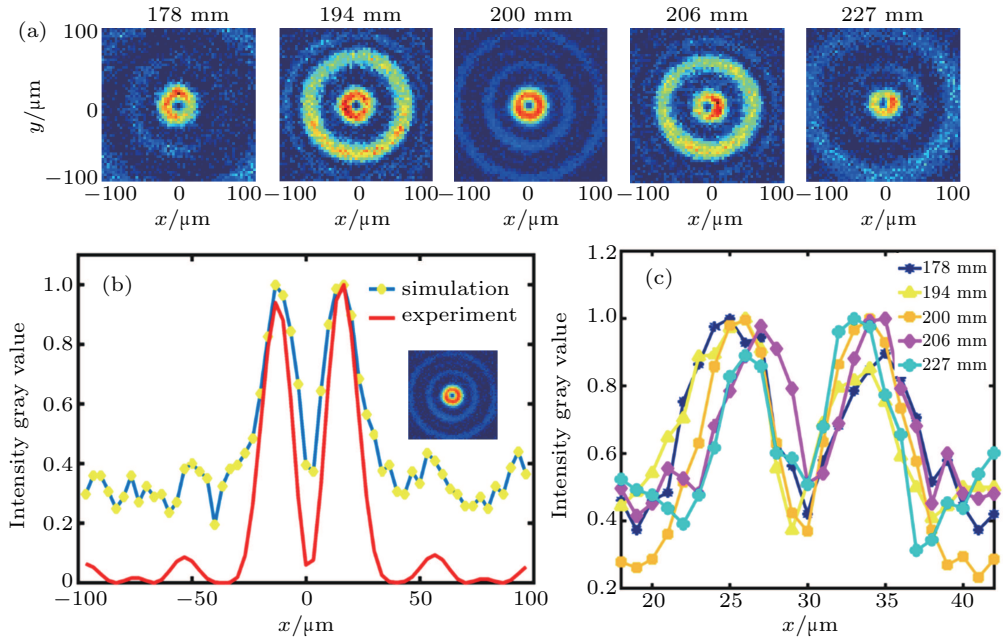


Fig. 6. (a) Intensity distribution of the main and subsidiary dark cores of FSZP, (b) detailed characteristics of main focus, (c) intensity profiles along x axis on main and subsidiary focal planes.

5. Conclusions

We propose FSZP as an alternative diffractive element for the generation of optical vortex beams with multiple foci. The focal depths and cross-section irradiances at different positions of the FSZP are simulated and the influences on the generated vortices with different TCs are discussed. As presented in this work, an FSZP with $p = 1$, $N = 2$, and $S = 4$ is fabricated by using the electron beam lithography. According to this, we also experimentally demonstrated the remarkable ability of FSZP to generate the sequence optical vortices with a larger depth of focus. One potential application of this new design with an increased depth of focus is its integration in a three-dimensional optical alignment system.[23] In addition, the FSZP may become a potential alternative to replace the conventional vortex array generators in the x-ray,[24] extreme ultraviolet,[25] and microwave[26] applications.

References

[1] Paterson L, MacDonald M P, Arlt J, Sibbett W, Bryant P E and Dholakia K 2001 *Science* **292** 912
[2] Daria V R, Rodrigo P J and Gluckstad 2004 *J. Appl. Phys. Lett.* **84** 323
[3] Wang Z X, Zhang N and Yuan X C 2011 *Opt. Express* **19** 482
[4] Moreno I, Davis J A, Pascoguin B M L, Mitry M J and Cottrell D M 2009 *Opt. Lett.* **34** 2927
[5] Chu S C, Chen Y T, Tsai K F and Otsuka K 2012 *Opt. Express* **20** 7128
[6] Shu J H, Chen Z Y, Pu J X and Liu Y X 2011 *Chin. Phys. B* **20** 114202
[7] Beijersbergen M, Coerwinkel R, Kristensen M and Woerdman J 1994 *Opt. Commun.* **112** 321
[8] Cheong W, Lee W, Yuan X C and Zhang L S 2004 *Appl. Phys. Lett.* **85** 5784
[9] Sakdinawat A and Liu Y 2007 *Opt. Lett.* **32** 2635
[10] Cojoc D, Kaulich B, Carpentiero A, Cabrini S, Businaro L and Fabrizio E 2006 *Microelectron. Eng.* **83** 1360
[11] Heckenberg N R, McDuff R C, Smith C P and White A G 1992 *Opt. Lett.* **17** 221
[12] Zhang N, Yuan X C and Burge R E 2010 *Opt. Lett.* **35** 3495
[13] Xavier J, Vyas S, Senthilkumaran P, Denz C and Joseph J 2011 *Opt. Lett.* **36** 3512
[14] Saavedra G, Furlan W D and Monsoriu J A 2003 *Opt. Lett.* **28** 971
[15] TaoS H, Yuan X C, Lin J and Burge R E 2006 *Appl. Phys. Lett.* **89** 031105
[16] Cheng S B, Zhang X Y, Ma W Z andTao S H 2016 *Sci. Rep.* **6** 34492
[17] Machado F J, Monsoriu J A and Furlan W D 2017 *Vortex Dynamics and Optical Vortices Hector Perez-de-Tejada* IntechOpen
[18] Yu J J, Zhou C H, Jia W, Hu A D, Cao W G, Wu J and Wang S Q 2012 *Appl. Opt.* **51** 6799
[19] Ji Z W, Zang H P, Fan C Z, Wang J, Zheng C L, Wei L, Wang C K and Cao L F 2018 *J. Opt. Soc. Am. A* **35** 726
[20] Li Z H, Zhang M N, Liang G T, Xing L, Chen X Y and Cheng C F 2013 *Opt. Express* **21** 15755
[21] Wei L, Gao Y L, Wen X L, Zhao Z Q, Cao L F and Gu Y Q 2013 *J. Opt. Soc. Am. A* **30** 233
[22] Xie C Q, Zhu X L, Shi L N and Liu M 2011 *Opt. Lett.* **351** 765
[23] Zhong W P and Belić M 2009 *Phys. Rev. A* **79** 23804
[24] Peele A G, Nugent K A, Mancuso A P, Paterson D, McNulty I and Hayes J P 2004 *J. Opt. Soc. Am. A* **21** 1575
[25] Hernández-García C, Picón A, Román J S and Plaja L 2013 *Phys. Rev. Lett.* **111** 083602
[26] Bothner D, Clauss C and Koroknay E 2012 *Appl. Phys. Lett.* **100** 012601